PHILIPPINE ENGINEERING JOURNAL
PEJ 2021; Vol. 42, No. 2: 1-24

Received: 02 February 2021
Accepted: 11 July 2021

Thermodynamic Performance Evaluation of Internal Heat Exchanger in a Compressor-Driven Ejector Heat Pump System

John Carlo S. Garcia* and Menandro S. Berana
Department of Mechanical Engineering, College of Engineering,
University of the Philippines, Diliman, Quezon City, 1101, Philippines
**Corresponding Author: jsgarcia1@up.edu.ph*

Abstract— *This study provides a theoretical analysis of the effect of internal heat exchanger (IHX) on an ejector heat pump system. An internal heat exchanger is placed between the intermediate-pressure and high-pressure sides of the system. The performance of the systems with and without IHX are evaluated using coefficient of performance and exergy efficiency. The results show that the ejector heat pump system with IHX has higher heating capacity, coefficient of performance, and exergy efficiency. The introduction of IHX also increases the reliability of the compressor by ensuring that only vapor refrigerant enters the component. The performance of five refrigerants, namely R32, R290, R407c, and R410a, are compared. Among the refrigerants observed, R134a has the highest coefficient of performance (7.17), while R32 has the highest exergy efficiency (68.73%). The effects of evaporating and condensing temperatures to the system with IHX are also investigated. It is found out that the evaporating temperature has a significant effect on both the coefficient of performance and exergy efficiency.*

Keywords— ejector, heat pump, COP, exergy analysis

I. INTRODUCTION

Improvement of system performance is commonly one of the main objectives of most studies on thermal systems. Power, refrigeration, and heat pump systems are often evaluated using energy-based or entropy-based analyses. Increasing the capacity of the system is observed in energy-based analyses, while minimizing the entropy generation or exergy destruction is desired in entropy-based analyses. Thermal and exergy efficiencies, and coefficient of performance (COP) are used as metrics in the assessment of a system's performance. Thermal efficiency of a power system measures the percentage of the heat energy converted to useful work. For a refrigeration or heat pump system, the COP is defined as the ratio of the cooling or heating capacity to the required work, respectively. On the other hand, exergy efficiency correlates both the quantity and quality of energy, and it denotes the utilization of available energy. The degree of irreversibilities of the processes in a system can also be measured using exergy efficiency [1]. For thermal systems with combined power and cooling or heating, exergy efficiency is often used over thermal efficiency [2-4].

Researchers have explored several approaches in enhancing thermal systems such as investigating the effects of different operating parameters [5-7], comparing working fluid performance [6,8-9], optimizing components [10,11], and modifying system configuration [12-14]. For refrigeration and heat pump systems, an example of a modification of the standard vapor compression cycle is the introduction of an ejector into the system.

An ejector is a mechanical device that utilizes fluid flow with high pressure and velocity to entrain a low-pressure fluid flow. The two flows mix, and the resulting stream is then expanded to an intermediate pressure. Due to their simplicity, reliability, and low cost and maintenance, ejector refrigeration systems have gained much attention among researchers [15,16]. Generally, ejector refrigeration systems are classified as heat-driven and compressor-driven systems. In a heat-driven ejector system, the ejector replaces the compressor, and a pump and a generator are introduced into the system. Meanwhile, throttling losses are minimized in a compressor-driven system. There have been numerous theoretical and experimental studies on the performance of ejector refrigeration systems.

Nehdi et al. [17] conducted theoretical analyses and simulation of a compressor-driven ejector refrigeration system and concluded that the ejector system yielded higher COP compared to a standard vapor compression cycle. They also observed that when the condenser temperature increased, the COP of the standard cycle decreased considerably more compared to the ejector system. Sarkar [18] compared the performance of three natural refrigerants in an ejector refrigeration system. The results showed that there were 26.1%, 22.8%, and 11.7% COP increase in systems using propane, isobutane, and ammonia, respectively. The study of Li et al. [19] showed that ejector-expansion refrigeration system using R1234f had a higher COP and volumetric cooling capacity compared with the standard refrigeration cycle. They also found out that the performance of the ejector system was better especially at higher condensing and lower evaporating temperatures. Generally, the increase in COP of ejector refrigeration systems is attributed to the recovery of the throttling losses in the standard vapor compression cycle. As a result, the pressure ratio of the compressor also decreases.

The trend of having a better performance than a standard vapor compression system is also observed for ejector heat pump systems. Banasiak et al. [20] conducted an experimental and numerical investigation of the optimum ejector geometry for a R744 heat pump. Their results showed that the maximum increase in COP of the ejector heat pump was 8% compared to a conventional expansion valve. The performance of a two-phase CO_2 ejector heat pump system was investigated by Taslimi Taleghani et al. [21]. They found out that the ejector improved the COP by up to 12% and increased the heating capacity by up to 25% compared to the standard cycle. For ejector heat pump systems, the minor improvement in COP is attributed to the increased mass flow rate at the compressor and the lower compressor pressure ratio. Although the increase in mass flow rate results in higher heating capacity, it would also increase the required compression work of the system.

Further improvement of ejector refrigeration and heat pump systems is studied in the recent years. There have been a multitude of theoretical studies optimizing the ejector geometry and exploring different refrigerants that would result in an improved system performance. However, only few have investigated the effect of introducing an internal heat exchanger in an ejector refrigeration or heat pump system. An internal heat exchanger (IHX) is added to the system to transfer heat between the high-pressure and low-pressure flows. In the standard vapor compression cycle, the exiting stream from the evaporator is preheated by exchanging heat with the exiting stream of the condenser. Studies show that the COP of the system with IHX is higher due to the increased cooling capacity [12,22]. Hence, the potential of ejector systems with internal heat exchanger is also explored.

Sarkar [18] studied the effect of using an IHX in the ejector expansion cycle. He inferred that the pressure lift ratio of the ejector decreased that resulted in a higher compression work and consequently a lower COP. He further concluded that the addition of IHX was not profitable for the system. Moles et al. [23] modified the compressor-driven ejector refrigeration system by introducing an IHX where the exit stream of the condenser exchanges heat with the vapor stream that exits the separator. Their results showed that the ejector system with IHX had a detrimental effect on the COP of the system. The modified system had an increased refrigerating effect only at higher IHX effectiveness, which resulted in an inadmissible values of compressor discharge temperature. Garcia and Berana [12] compared the performance of internal heat exchanger in a standard refrigeration with an ejector refrigeration system. Based on their simulations, the internal heat exchanger had a positive effect on the system performance of a standard refrigeration cycle, while it resulted in a lower COP for an ejector system. They further concluded that the IHX mainly functioned as a safeguard to ensure that only superheated vapor enters the compressor. Rodriguez-Muñoz [13] suggested a different configuration of ejector-IHX system compared to the system investigated by Moles et al. [23], and Garcia and Berana [12]. In their configuration, the IHX was placed between the condenser and evaporator outlets. Their configuration also resulted in a decrease in COP, but the maximum exergy efficiency was reached at an IHX effectiveness of 20%. It is evident that from these studies that the ejector-IHX compressor system does not improve the COP. However, there are less available information on the performance of ejector heat pump systems with internal heat exchanger (ICDEHP).

In this study, a theoretical analysis of the performance of ICDEHP system was conducted. The internal heat exchanger was used to superheat the vapor exiting the separator by transferring heat from the exit stream of the condenser. The ICDEHP system was evaluated using COP and exergy efficiency, and it was compared to the performance of a standard ejector heat pump. The performance of five working fluids— R32, R134a, R290 (propane), R407c, and R410a— were also explored. Moreover, parametric analysis was conducted to investigate the effects of the heat transfer ratio (HTR) of the IHX, condensing temperature, and evaporating temperature on the performance of the system.

II. SYSTEMS DESCRIPTION

The effect of the internal heat exchanger (IHX) on the system performance was primarily observed in this study, having the ejector heat pump as the baseline of comparison. In this study, the following systems were analyzed: (a) compressor-driven ejector heat pump (CDEHP), and (b) CDEHP with IHX (CDEHP-IHX).

2.1. Compressor-Driven Ejector Heat Pump

In an ejector heat pump system, as illustrated in Figure 1, the saturated mixture coming from the ejector (state 1) is separated to saturated vapor and saturated liquid. The saturated vapor refrigerant (state 2) is compressed to the condensing pressure and exits as superheated vapor (state 3). It is then cooled (state 4) as it exchanges heat with an external fluid at the condenser. On the other hand, the saturated liquid (state 6) that comes from the vapor-liquid separator is throttled to the evaporating pressure (state 7). The refrigerant is then vaporized (state 8) as it absorbs heat from the environment at the evaporator.

The exiting flows from the condenser and evaporator become the primary and secondary flows of the ejector, respectively. The high-pressure saturated liquid (state 4) passes through the converging-diverging nozzle (state 5), which then entrains the low-pressure fluid (state 9). The two flows are assumed to mix at a constant pressure in the mixing chamber (state 10). The resulting flow then recovers pressure as it passes through the diffuser (state 1), thus, completing the cycle.

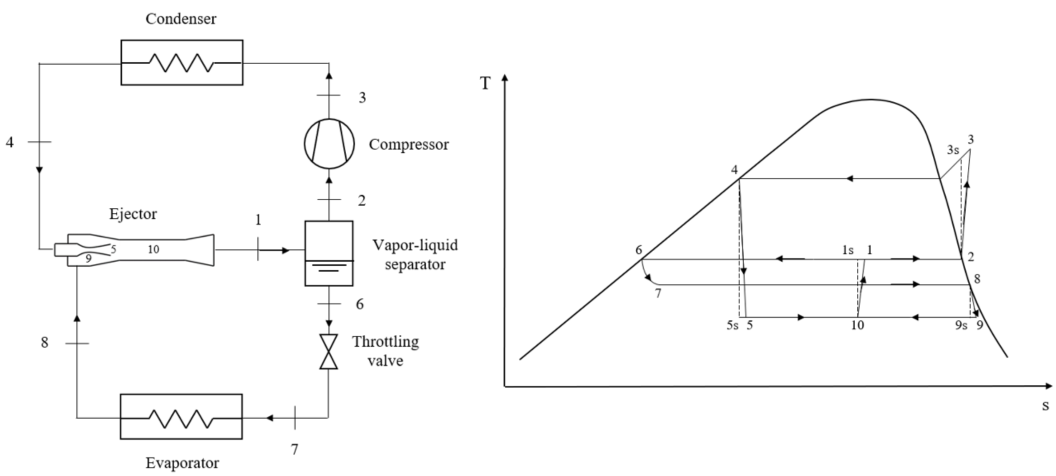

Figure 1. Schematic and *T-s* diagrams of a compressor-driven ejector heat pump

2.2. CDEHP with Internal Heat Exchanger (ICDEHP)

An internal heat exchanger is introduced in the ejector heat pump system and is placed between the intermediate-pressure (ejector and vapor-liquid separator) and high-pressure sides (condensing unit) of the cycle. Figure 2 shows the schematic diagram of the CDEHP system with an internal heat exchanger.

The saturated vapor (state 12) that flows out of the vapor-liquid separator is preheated at the internal heat exchanger using the sensible heat of condenser subcooling. The resulting superheated vapor refrigerant (state 13) then flows through the compressor where its pressure is elevated to the condensing pressure (state 14). The superheated working fluid desuperheats and condenses to saturated liquid (state 15) as it gives off heat to the heated space. It is further subcooled (state 16) in the internal heat exchanger before entering the ejector.

The pressure of the saturated liquid refrigerant (state 18) drawn from the separator is lowered as it passes through the throttling device (state 19). It is then heated to saturated vapor (state 20) at the evaporator. This low-pressure saturated vapor is entrained (state 20) by the high-pressure subcooled liquid as it passes through the motive nozzle (state 17). These two streams then mix (state 22), and the resulting stream recovers pressure at the diffuser (state 11). The exiting stream of the ejector goes to the vapor-liquid separator.

One of the key differences of an ejector heat pump with IHX is that the primary flow enters the ejector at a lower temperature. It is due to the subcooling at the condenser, and the utilization of the sensible heat at the internal heat exchanger.

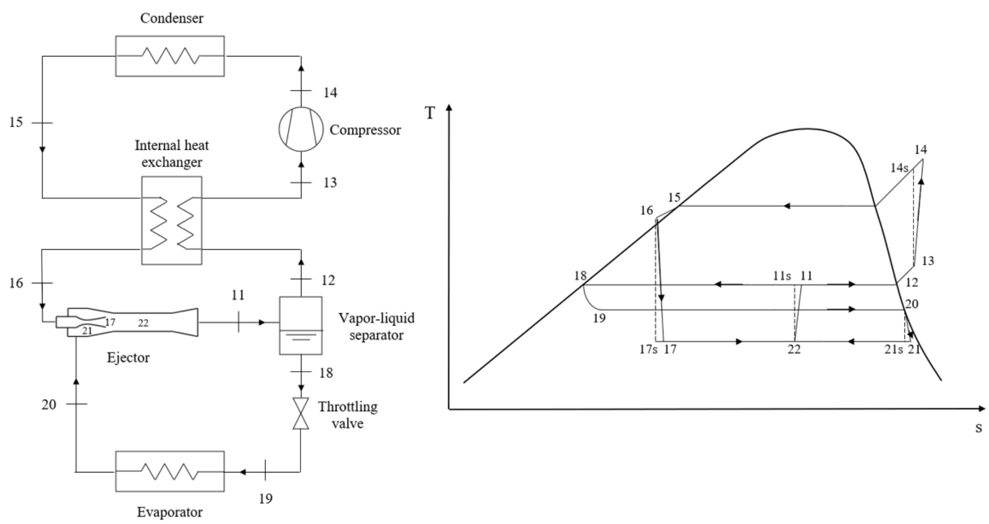

Figure 2. Schematic and *T-s* diagrams of an ICDEHP system

2.3. Refrigerant Selection

The five refrigerants under consideration were R32, R134a, R290 (propane), R407c, and R410a. These refrigerants are some of the commonly used working fluids for heat pump systems, especially for industrial applications [24]. They were also chosen for their thermodynamic properties and environmental compatibility, which are summarized in Table 1 [25,26].

Table 1. Refrigerant Properties

Property	R32	R134a	R290	R407c	R410a
Critical temperature (^oC)	78.35	101.1	96.7	86.74	72.13
Critical pressure (bar)	58.16	40.67	42.48	46.2	49.26
Flammability	low	no	high	no	no
ODP	0	0	0	0	0
GWP	675	1430	3	1774	2088
Toxicity (ppm)	no	no	2100	1000	1000

2.4. Operating Conditions

The assumed values of each operating parameter are listed in Table 2.

Table 2. Assumed conditions of system parameters

Environment temperature	T_o = 30 °C
Environment pressure	P_o = 101.325 kPa
Condensation temperature	T_k = 60 °C
Evaporation temperature	T_e = 25 °C
Motive nozzle isentropic efficiency	η_{mn} = 0.85 [13, 17-19]
Suction nozzle isentropic efficiency	η_{sn} = 0.85 [13,17-19]
Mixing section isentropic efficiency	η_{ms} = 0.95 [13,17-19]
Diffuser isentropic efficiency	η_d = 0.85 [13,17-19]

For the ejector modeling equations, the pressure difference between the evaporating pressure and the ejector mixing section pressure Δp is needed. **Figure 3** shows the variation of the system's coefficient of performance (COP) with Δp at the given operating conditions. The COP of the CDEHP system was numerically calculated at a Δp from 5 to 100 kPa, with increments of 5 kPa. For both configurations, the Δp that yielded the highest COP was used.

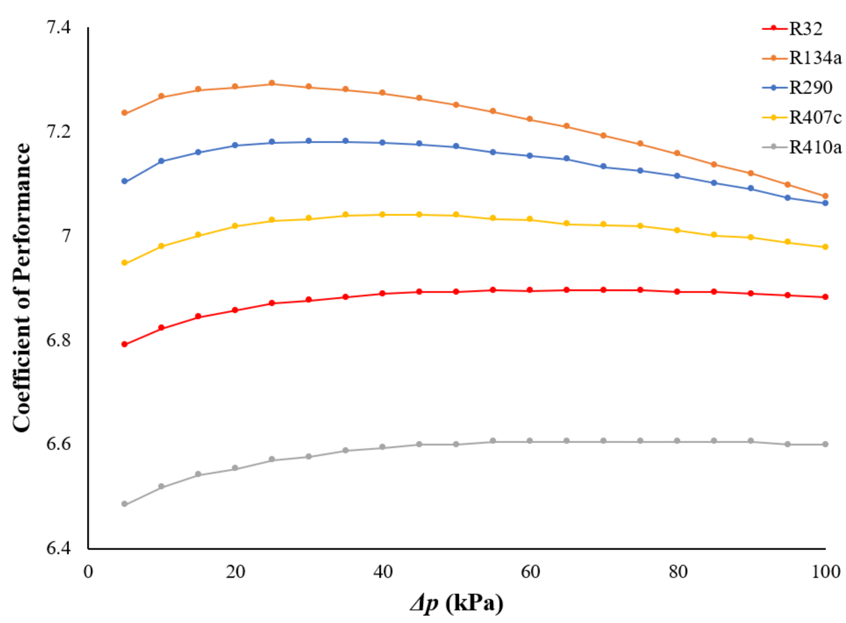

Figure 3. Optimal pressure difference between evaporator and ejector mixing pressures

III. SYSTEM MODELING EQUATIONS

The following assumptions are made for the system simulation:

(1) The system is at steady-state conditions.
(2) The difference in the kinetic and potential energies as well as pressure drops in pipes are neglected. Heat losses at the condenser, compressor, ejector, evaporator, internal heat exchanger, throttling device, and vapor-liquid separator are also considered negligible.
(3) The throttling process is isenthalpic.
(4) The stream of working fluid that exits the evaporator is saturated vapor. For the ejector heat pump system, the refrigerant exits the condenser as saturated liquid.
(5) The exit states at the vapor-liquid separator are saturated.

For the ejector modeling equations, the calculation approach of Li et al. [19] is used with the following assumptions:

(1) One-dimensional, homogeneous flow is considered.
(2) The inlet and exit velocities are negligible.
(3) The primary and secondary flows are at the same pressure before entering the constant area mixing region.
(4) Friction losses in the ejector are accounted in terms of the motive nozzle, suction nozzle, mixing section, and diffuser efficiencies.

The entrainment ratio of the ejector is defined as the ratio of the mass flow rate of the secondary flow to the mass flowrate of the primary flow, or is given as

$$\mu = \frac{\dot{m}_{sf}}{\dot{m}_{pf}} \tag{1}$$

For both configurations, the primary flow of the system goes to the high-pressure loop, while the secondary flow goes to the low-pressure loop.

Applying the system assumptions and the law of conservation of energy at each component of ICDEHP, the following equations are obtained:

- For the compressor,

$$w_c = \frac{h_{14} - h_{13}}{1 + \mu} \tag{2}$$

$$\eta_c = \frac{h_{14s} - h_{13}}{h_{14} - h_{13}} = 0.874 - 0.0135 \left(\frac{p_{dis}}{p_{suc}}\right) \tag{3}$$

- For the condenser,

$$q_k = \frac{h_{14} - h_{15}}{1 + \mu} \tag{4}$$

- For the internal heat exchanger,

$$\mathrm{HTR} = \frac{h_{13} - h_{12}}{h_{15} - h_{16}} \tag{5}$$

- For the vapor-liquid separator,

$$(1 + \mu)h_{11} = h_{12} + \mu h_{18} \tag{6}$$

- For the throttling valve,

$$h_{18} = h_{19} \tag{7}$$

- For the evaporator,

$$q_e = \frac{\mu(h_{20} - h_{19})}{1 + \mu} \tag{8}$$

For the compressor efficiency η_c, the empirical relation proposed by Brunin et al. [27] was used. The energy equations for the ejector heat pump system is analogous with the equations of the ICDEHP system. Meanwhile, the heat transfer ratio (HTR) is used for the internal heat exchanger where it measures the amount of heat that is transferred from the hotter to the cooler fluid stream.

The performance of system of both heat pump configurations is evaluated by the coefficient of performance (COP) and exergy efficiency η_{exg}. The COP is based on the first law of thermodynamics and is defined as the ratio of the useful energy to the input energy. For heat pump systems, it is given by

$$COP = \frac{q_k}{w_c} \tag{9}$$

Exergy efficiency is defined as the ratio of the exergy output to the exergy input. In both configurations, the exergy input of the system is the specific work of the compressor, while the exergy output is taken as the exergy of heating that is measured at the condenser. Hence, the exergy efficiency is expressed as

$$\eta_{exg} = \frac{e_k}{w_c} \tag{10}$$

It is also important to note the exergy destruction of each component in evaluating the performance of the system. The performance of a component can be improved by optimizing its design or determining the optimal working parameters. To measure the exergy destruction, the specific exergy of each state point must be first calculated, and it is given by

$$e_n = (h_n - h_o) - T_o(s_n - s_o) \tag{11}$$

In this study, the reference pressure p_o and temperature T_o are the specified dead states. Moreover, the following assumed in the exergy analysis:

(1) Only physical exergies are accounted for the stream flows.
(2) Chemical, kinetic, and potential exergies are neglected.

Thus, with the given assumptions, the specific exergy balance in each component is expressed as

$$i = \sum e_{in} - \sum e_{out} \tag{12}$$

where *i* is the specific exergy destruction. The specific exergy destruction for each component is given by

- For the compressor,
$$i_c = e_{13} + w_c - e_{14} \tag{13}$$
- For the condenser,
$$i_k = e_{14} - e_{15} \tag{14}$$
- For the internal heat exchanger,
$$i_{IHX} = e_{12} + e_{15} - e_{13} - e_{16} \tag{15}$$
- For the ejector,
$$i_j = e_{16} + e_{20} - e_{11} \tag{16}$$
- For the throttling valve,
$$i_t = e_6 - e_7 \tag{17}$$
- For the evaporator,
$$i_e = e_{19} - e_{20} \tag{18}$$

Assuming negligible heat loss and friction losses at the vapor-liquid separator, there would be no exergy destruction. Hence, the specific exergy of the flow that goes in the component is equal to the sum of the specific exergies of the saturated liquid and vapor flows.

The solution procedure for evaluating the system performance is shown in Figure 4. Refrigerant properties were obtained using the values from REFPROP [28]. The values of error used for finding the degree of subcooling and the entrainment ratio μ were 0.001 kJ/kg and 0.0001, respectively.

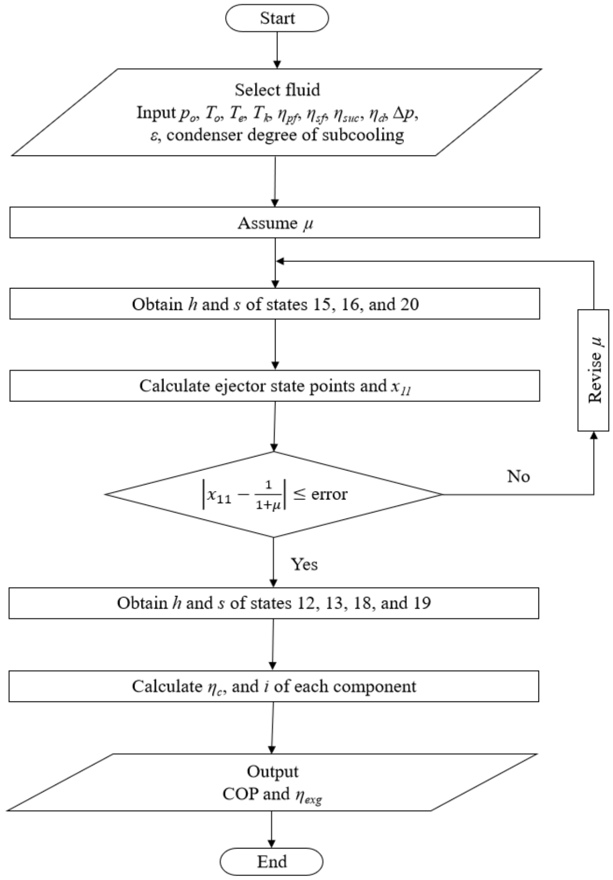

Figure 4. Simulation flowchart of system performance evaluation

IV. RESULTS AND DISCUSSION

The performance of the compressor-driven heat pump with internal heat exchanger was evaluated at condenser degree of subcooling of 1-10 ^oC, with increments of 1 ^oC. In refrigeration systems, operating up to 10 ^oC of subcooling is the most common. Since the evaporating and condensing temperatures were assumed to be constant, it is expected that the increase in the degree of subcooling results in the increase of the entrainment ratio. The influence of the condenser degree of subcooling on the entrainment ratio is seen in Figure 5.

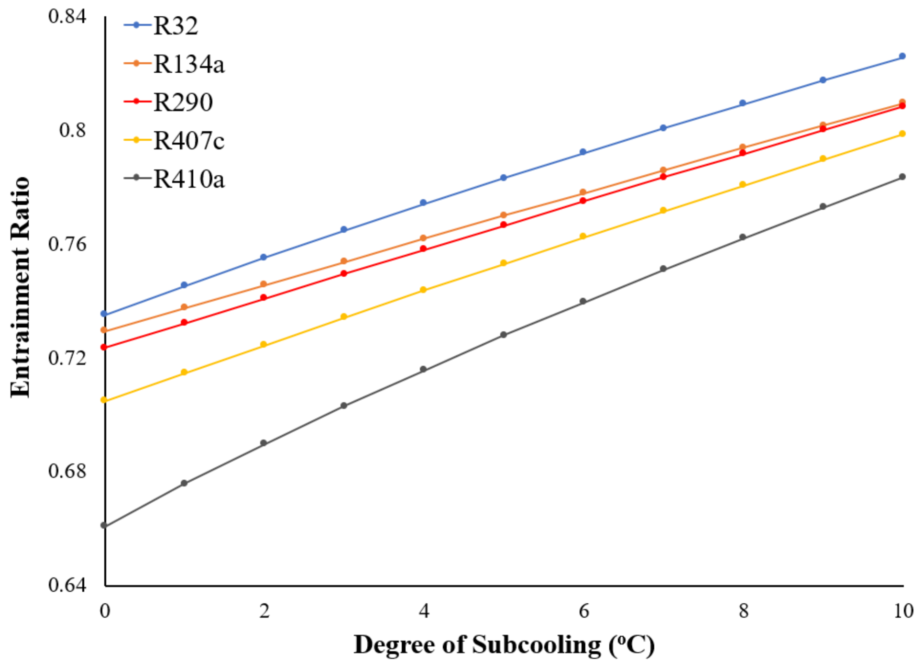

Figure 5. Effect of condenser degree of subcooling on the entrainment ratio

4.1. Effect on the Coefficient of Performance

One of the performance evaluators used in this study is the coefficient of performance. Figures 6 to 8 show the effect of the internal heat exchanger heat transfer ratio and condenser degree of subcooling on the heating effect, required compressor work, and COP of a R134a system. Higher degrees of subcooling resulted in lower pressure lift ratio of the ejector, which is caused by having lower static enthalpy of the primary flow. As the ejector pressure lift ratio decreased, the required compressor work increased. The increase of heating capacity with the increase in degree of subcooling is attributed to the higher compressor outlet temperature. On the other hand, higher heat transfer ratio indicated better heat exchange between the condenser outlet line and the compressor suction line, and the vapor refrigerant is preheated to a higher temperature. This resulted in a greater compressor work due to a higher specific volume of refrigerant that enters the compressor. In effect, the heating capacity also increased because the refrigerant exits the compressor at a higher temperature. Based on Figure 8, the COP increased with the heat transfer ratio and decreased with the degree of subcooling. The degree of subcooling had greater effect on the COP compared with the heat transfer ratio for it directly affects the ejector performance. At lower degrees of subcooling, the effect of HTR on COP became insignificant.

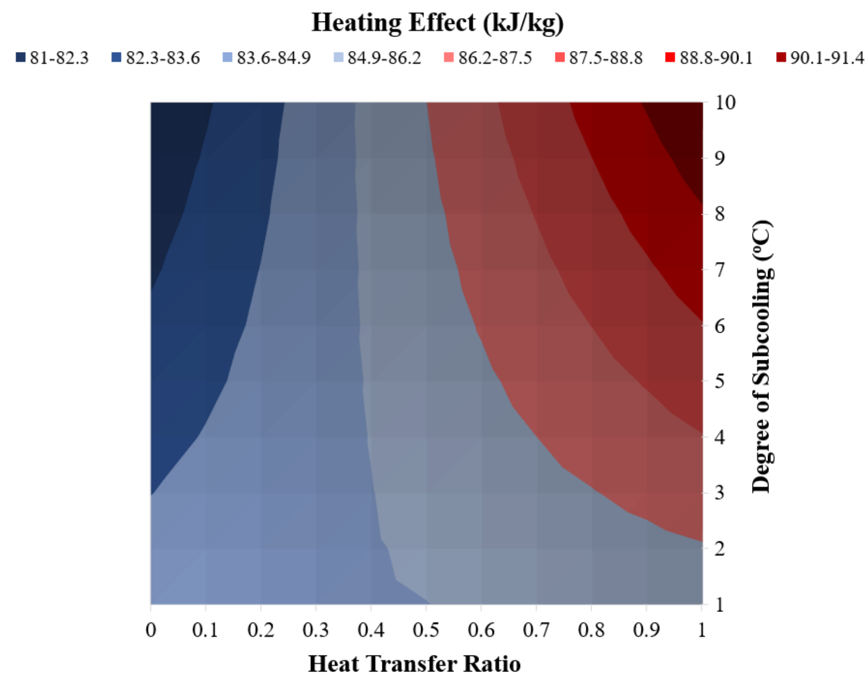

Figure 6. Effect of IHX HTR and condenser degree of subcooling on the heating effect of a R134 ICDEHP system

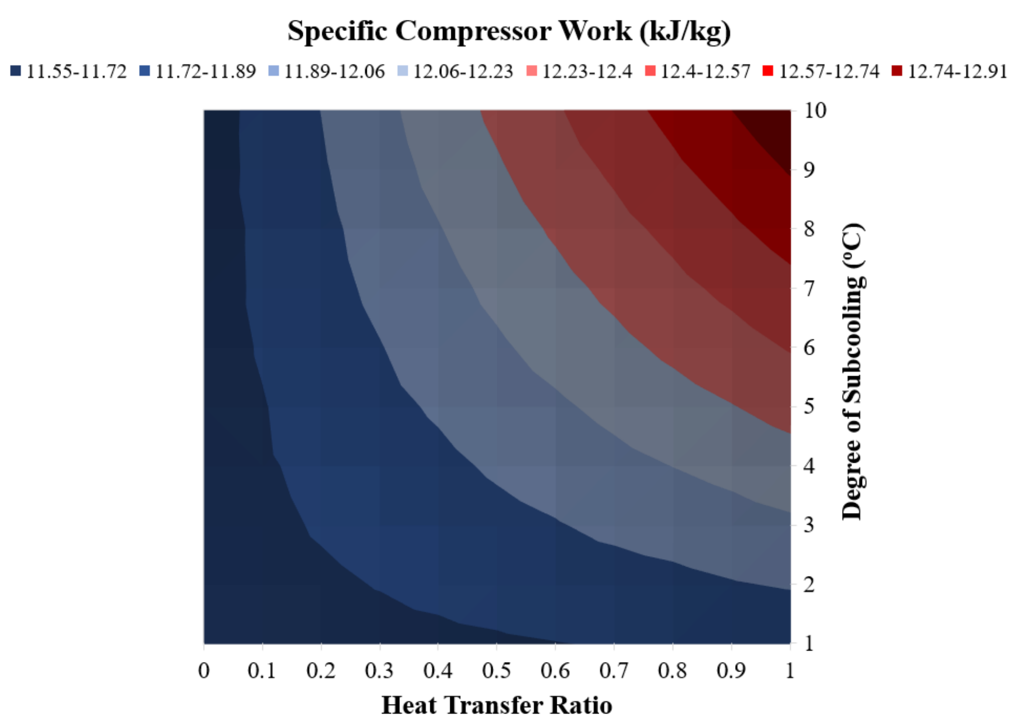

Figure 7. Effect of IHX HTR and condenser degree of subcooling on specific compressor work of a R134 ICDEHP system

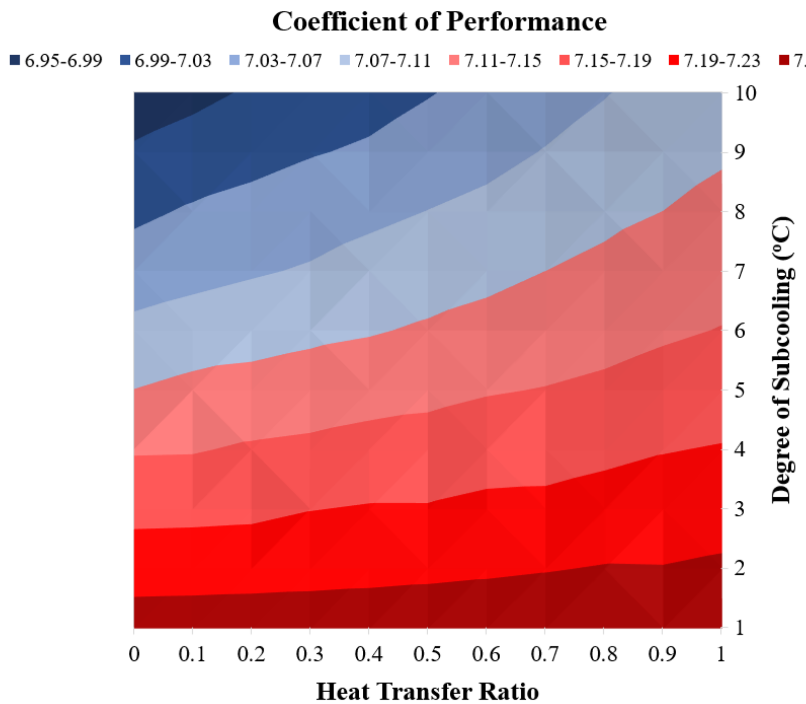

Figure 8. Variation of COP with IHX HTR and condenser degree of subcooling of a R134 ICDEHP system

4.2. Effect on the Exergy Efficiency

Another method of evaluating the performance of the system is by using exergy efficiency. Some studies prefer exergy analysis that using the first law efficiency since the former accounts the quality of energy transferred.

Figure 9 shows the effect of the internal heat exchanger heat transfer ratio and condenser degree of subcooling on the exergy efficiency of the system. At a given degree of subcooling, it was observed that exergy efficiency slightly improved with the increase in the IHX heat transfer ratio. Conversely, the exergy efficiency decreased with the increase in the degree of subcooling at a given HTR. However, a change in this trend between exergy efficiency and degree of subcooling was seen at high values of HTR. At HTR values of 0.8 to 1, the exergy efficiency increased with the degree of subcooling. This behavior is attributed to the change in the heating exergy and specific compressor work. Even though both heating exergy and specific compressor work increased with degree of subcooling, the change in the increase of compressor work decreased as compared with the significant increase in the heating exergy. It was also noted that the change in the degree of subcooling had a greater effect on the exergy efficiency that the IHX HTR.

Among the components of the system, the compressor and evaporator had the highest exergy destruction. The exergy destruction of both devices also increased with the degree of subcooling. The increase in the exergy destruction of the evaporator was caused by the increase of the entrainment ratio with the degree of subcooling. As the entrainment ratio increased, the refrigerant flow on the low-pressure side was also increased. The rise in exergy destruction of the compressor is attributed to the higher inlet temperature of the refrigerant and higher compression work.

On the other hand, the exergy destruction of ejector decreased with the degree of subcooling. Both the inlet temperature of the primary flow and the exit ejector flow decreased as a consequence of having higher degree of subcooling. It was also observed that the exergy destruction of the internal heat exchanger increased with degree of subcooling, which is attributed to the increase in the subcooling of the condenser exit flow and the superheating of the compression suction flow. Lastly, the expansion device experienced the least exergy destruction, which only accounted for 0.3% of the total exergy input.

The heat transfer ratio had a little to no effect on the exergy destruction of each component at a given degree of subcooling. The exergy destruction of the ejector, evaporator and expansion device was unaffected by HTR for their states remained the same. For the compressor and internal heat exchanger, there was an insignificant increase in the exergy destruction as the HTR increased.

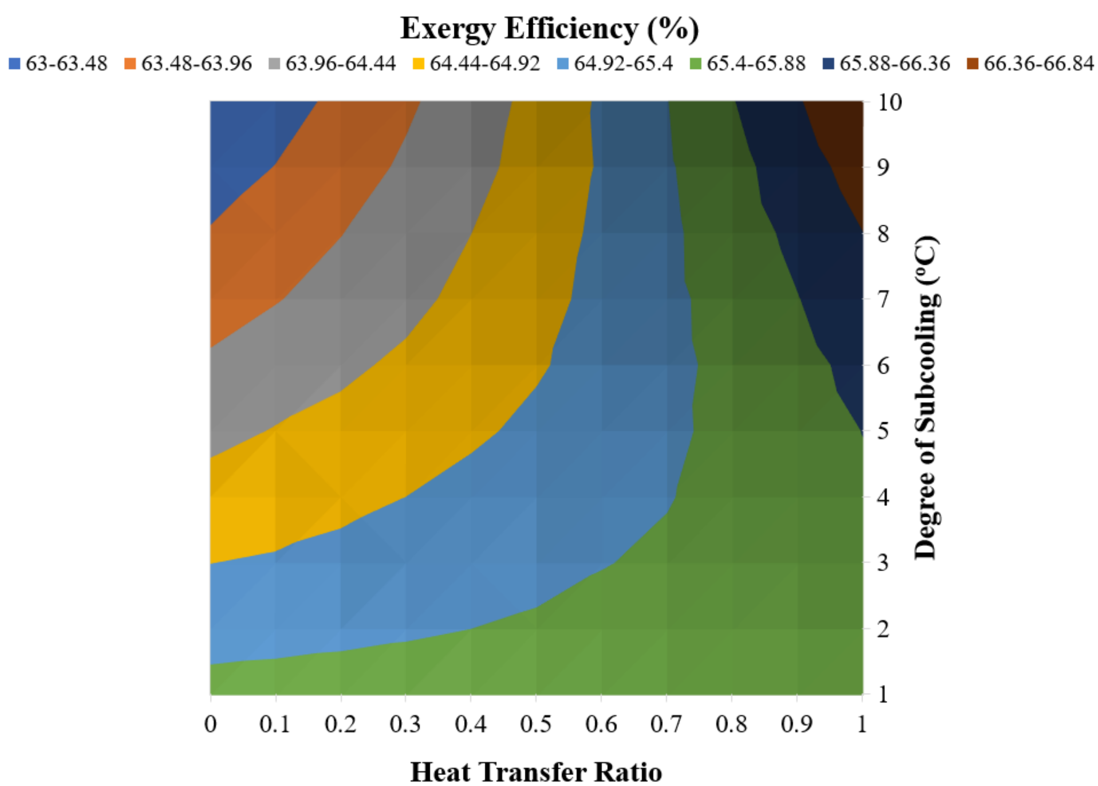

Figure 9. Variation of exergy efficiency with IHX HTR and condenser degree of subcooling of a R134 ICDEHP system

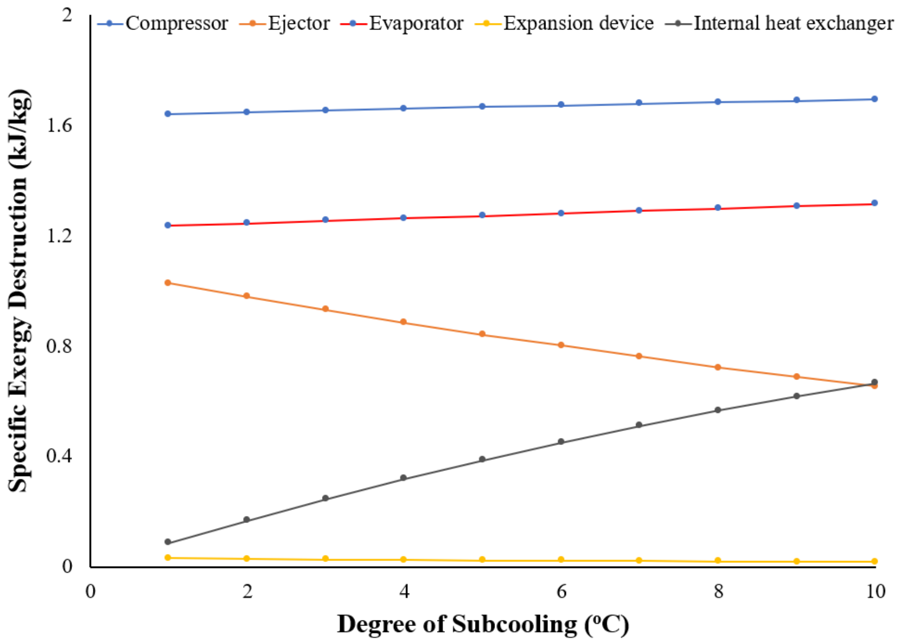

Figure 10. Effect of condenser degree of subcooling on the exergy destruction of each device in a R134 ICDEHP system with IHX ITR of 0.5

2.3. Comparison of Refrigerants

Among the five refrigerants, the system that uses R290 had the highest heating effect, and R134a had the highest coefficient of performance as seen in Figures 11 to 12. The results agreed with the general trend in comparing refrigerants through theoretical analysis. Low-pressure refrigerants outperform high-pressure refrigerants for the system is operating below their critical temperatures. It was also seen in Figure 12 that R32 had a different COP trend compared to the four refrigerants. This is attributed to the thermophysical properties of R32 being a pure wet fluid, whereas R134a and R290 are pure isentropic fluids.

The system with the highest exergy efficiency was the one using R32, as shown in Figure 13. It was also observed across five refrigerants that there was an increase in exergy efficiency at higher values of heat transfer ratio. Moreover, ICDEHP systems using R32 and R410a experienced greater increase in exergy efficiency than the other three refrigerants.

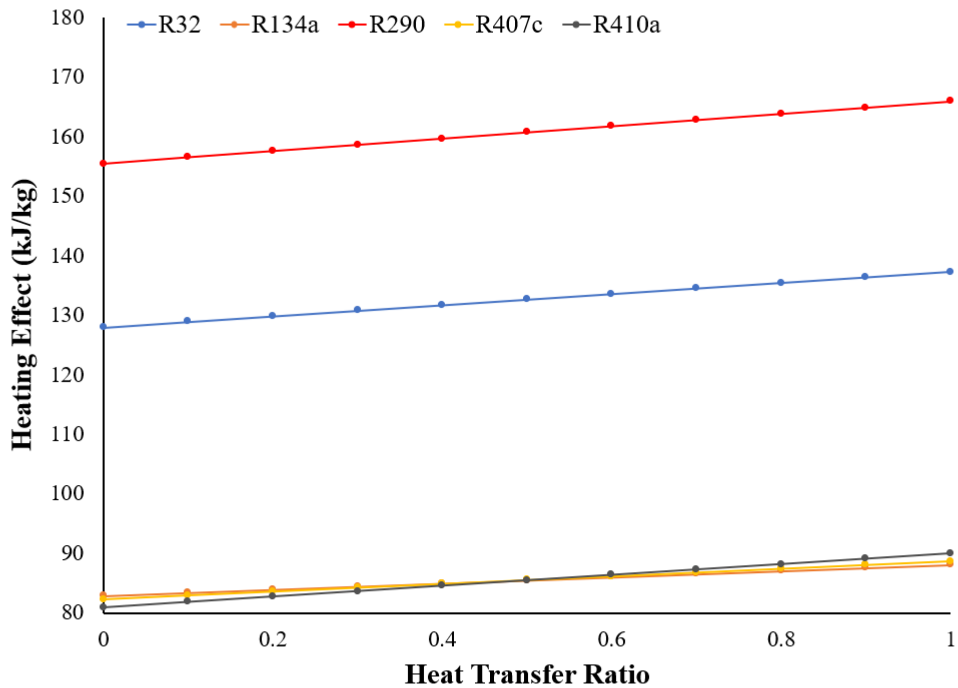

Figure 11. Comparison of heating effect of the five refrigerants at 5 ^{o}C subcooling

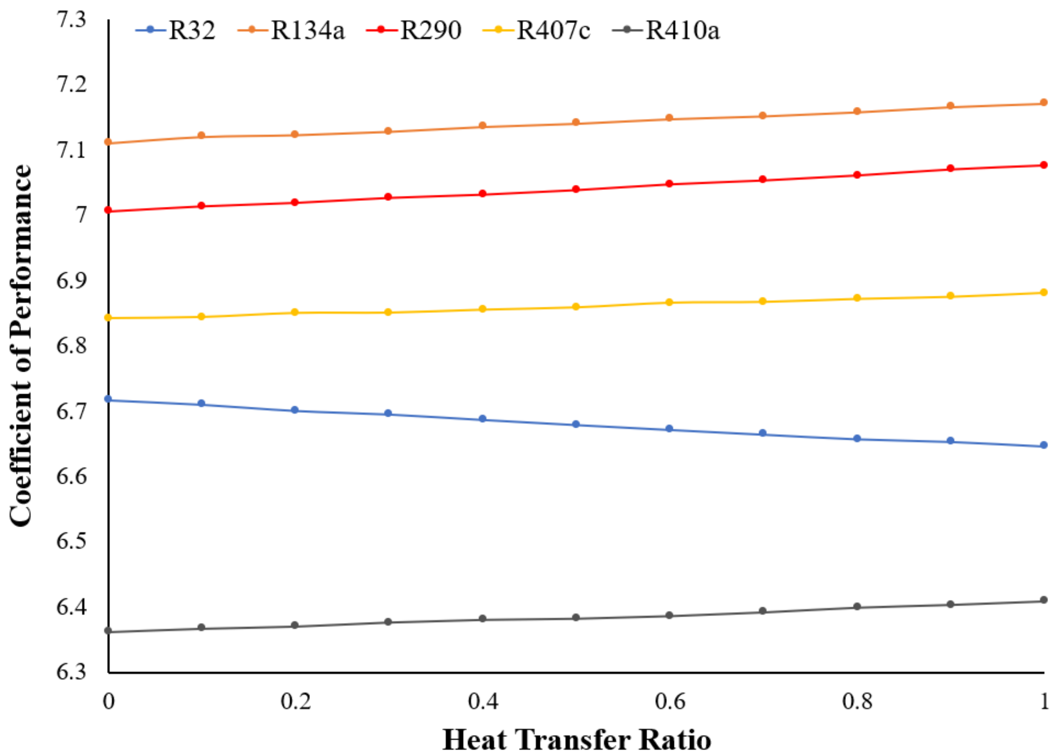

Figure 12. Comparison of COP of the five refrigerants at a HTR at 5 ^{o}C subcooling

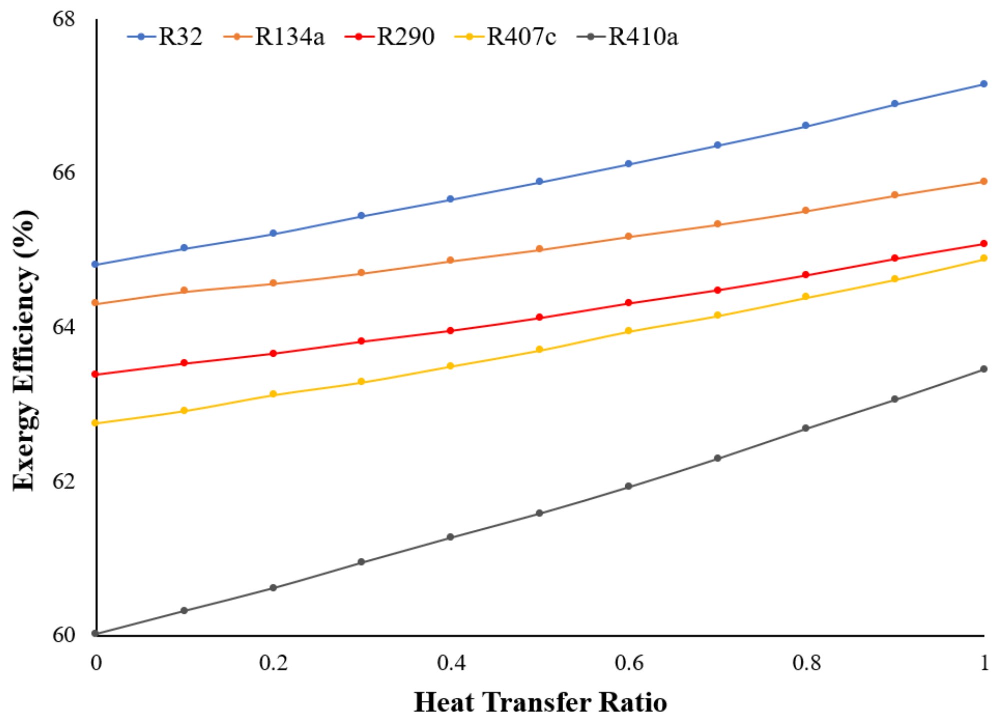

Figure 13. Comparison of exergy efficiency of the five refrigerants at 5 °C subcooling

2.4. Effect of Evaporating Temperature

Figures 14 to 16 illustrates the effect of the evaporating temperature and IHX heat transfer ratio on the heating effect, coefficient of performance, and exergy efficiency of the system. The heating effect decreased with the increase in the evaporator temperature. Conversely, both the coefficient of performance and exergy efficiency improved with rise in evaporating temperature. As the evaporating temperature increased, the entrainment ratio also increased. Consequently, this improved the pressure lift ratio of the ejector, which also reduced the compressor work.

It was also observed that the heat duty significantly varies with the IHX effectiveness as compared with the change brought about by the evaporating temperature. On the other hand, the COP and exergy efficiency greatly improved with the increase of the evaporating temperature.

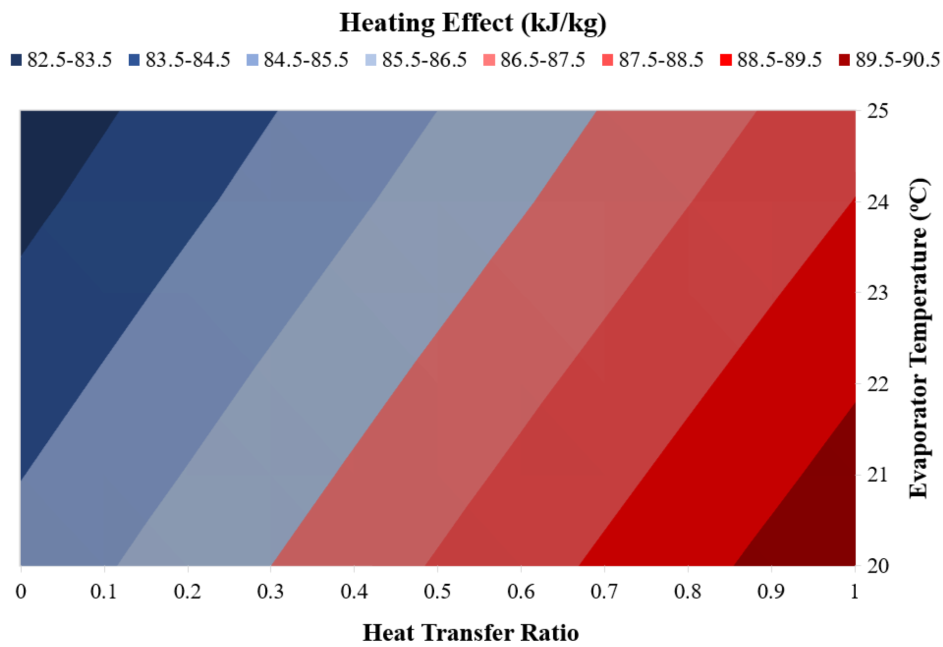

Figure 14. Effect of evaporator temperature and IHX HTR on heating effect of a R134a ICDEHP system at 5 °C subcooling

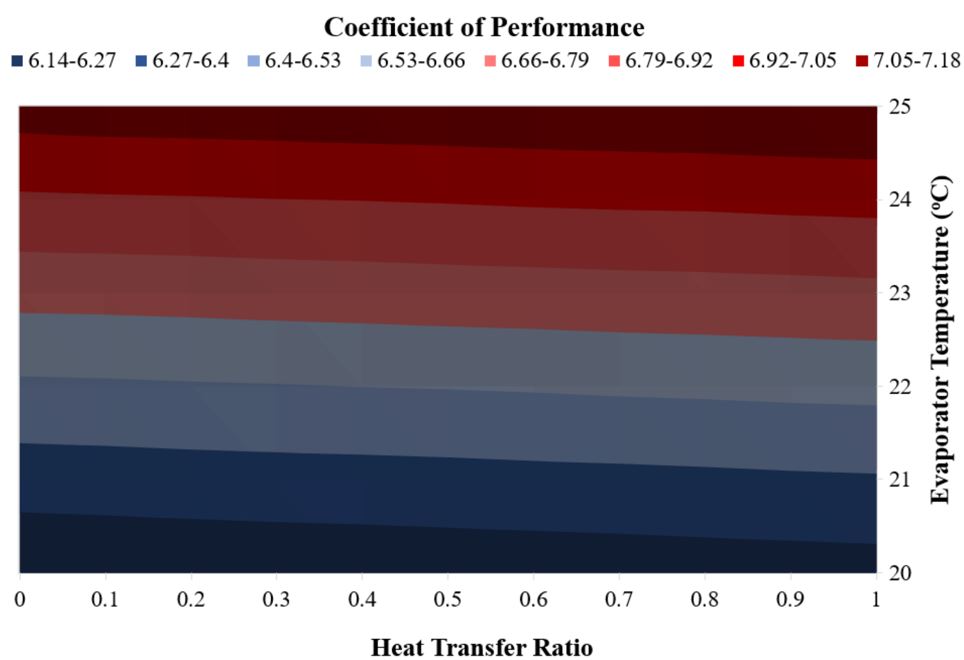

Figure 15. Effect of evaporator temperature and IHX HTR on COP of a R134a ICDEHP system at 5 °C subcooling

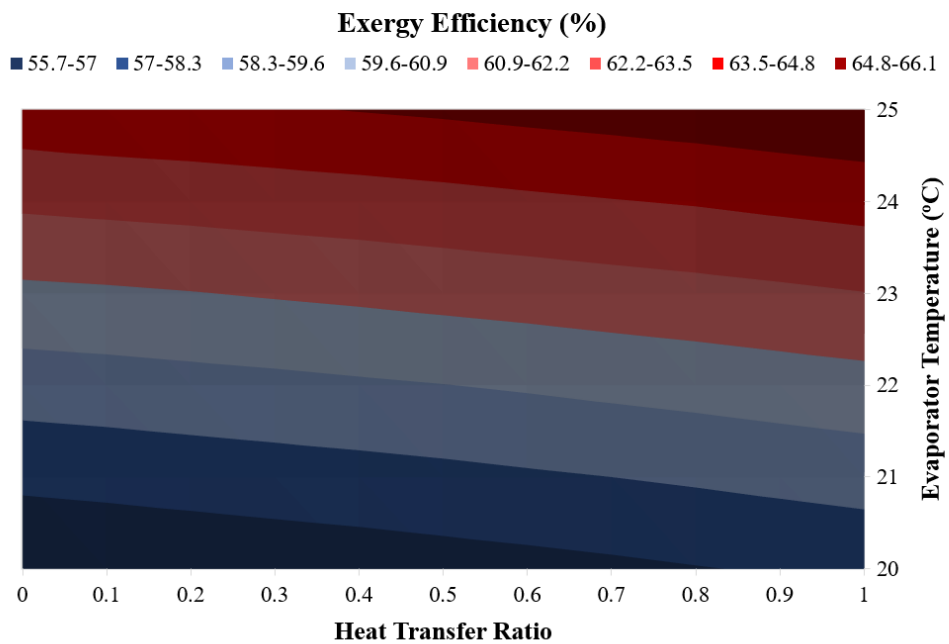

Figure 16. Effect of evaporator temperature and IHX HTR on η_{exg} of a R134a ICDEHP system at 5 ^{o}C subcooling

2.5. Effect of Condensing Temperature

The influence of the condensing temperature and IHX heat transfer ratio on the system performance is shown in Figures 17 to 19. The heating effect and exergy efficiency slightly decreased with the increase in condenser temperature; on the other hand, the coefficient of performance significantly worsened. Higher condensing temperature resulted in a higher entrainment ratio that lowered the heating effect and heating exergy of the condenser due to a decreased flowrate. This also resulted in a higher compressor work.

To improve the heating effect and exergy efficiency of the system, it is better to increase the IHX heat transfer ratio rather than having lower condenser temperature. In consequence, the coefficient of performance would also increase with the IHX heat transfer ratio.

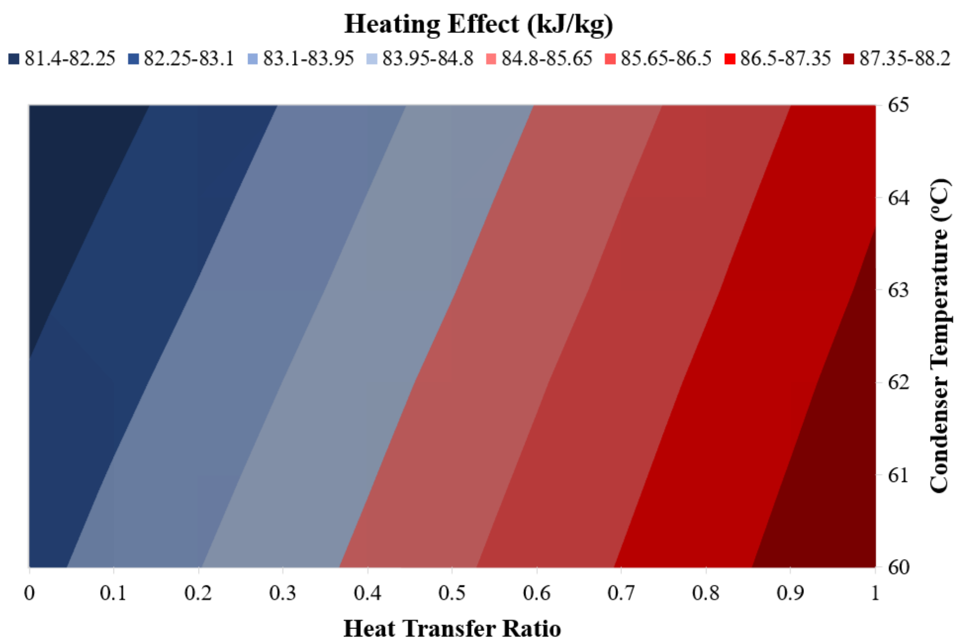

Figure 17. Effect of condenser temperature and IHX HTR on heating effect of a R134a ICDEHP system at 5 ^{o}C subcooling

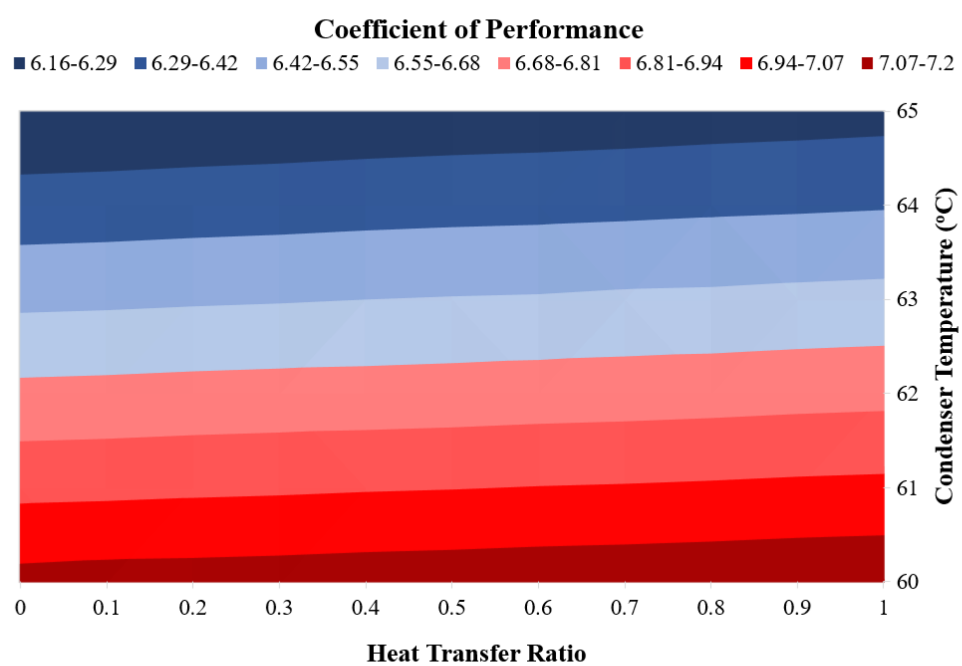

Figure 18. Effect of condenser temperature and IHX HTR on COP of a R134a ICDEHP system at 5 ^{o}C subcooling

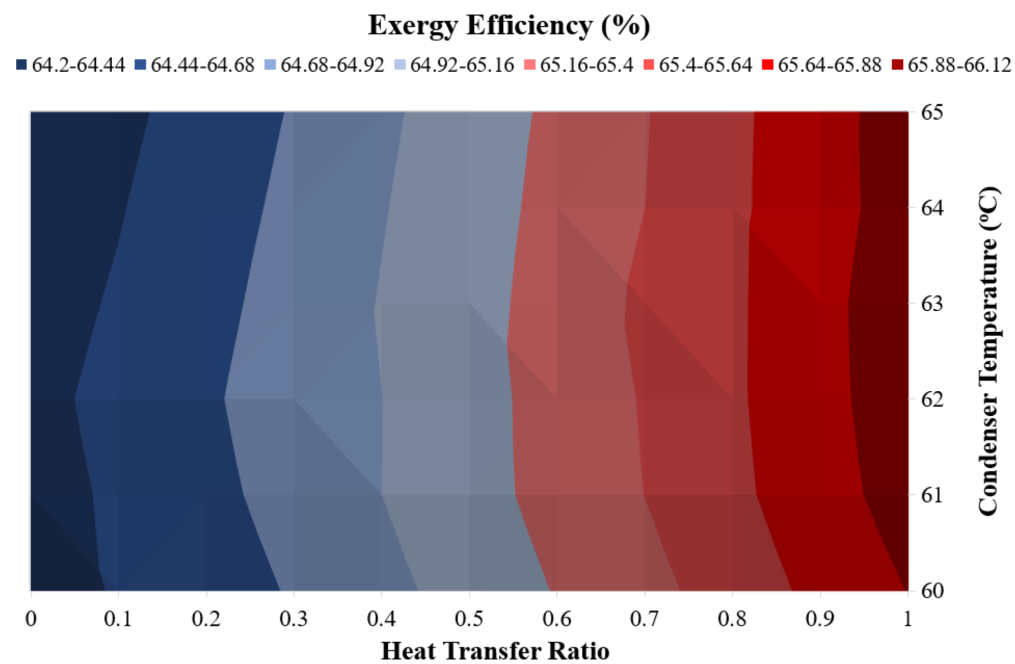

Figure 19. Effect of condenser temperature and IHX HTR on η_{exg} of a R134a ICDEHP system at 5 ^oC subcooling

V. CONCLUSION

The effect of introducing an internal heat exchanger in an ejector heat pump system was investigated. The performance of the system with and without an internal heat exchanger was theoretically evaluated by coefficient of performance and exergy efficiency. It was found out that the ICDEHP has slightly higher COP and exergy efficiency. Generally, the addition of internal heat exchanger improved the heating effect of the system and ensured that only vapor refrigerant enters the compressor.

The performance of five refrigerants were also compared. For both systems considered, R134a had the highest COP (7.17) and R32 had the highest exergy efficiency (68.73%), while the system using R410a performed the least with COP and exergy efficiency of 6.21 and 59.13%, respectively.

It was also concluded that the COP of a ICDEHP was significantly affected by the evaporator and condenser operating temperatures rather than the IHX heat transfer ratio. Moreover, the exergy efficiency greatly improved with higher evaporating temperature. Among the components of the system, it was found out that the compressor and evaporator had the largest values of exergy destruction.

NOMENCLATURE

COP	coefficient of performance
e	specific exergy (kJ kg^{-1} K^{-1})
h	specific enthalpy (kJ kg^{-1})
i	specific exergy destruction (kJ kg^{-1} K^{-1})
HTR	heat transfer ratio
ICDEHP	compressor-driven ejector heat pump with internal heat exchanger
IHX	internal heat exchanger
$\dot{m}$	mass flow rate (kg s^{-1})
p	pressure (kPa)
Δp	pressure drop (kPa)
q	specific heat (kJ kg^{-1})
s	specific entropy (kJ kg^{-1} K^{-1})
T	temperature (K)
w	specific work (kJ kg^{-1})

Greek symbols

η	efficiency
μ	entrainment ratio

Subscripts

1, …, 22	state points
c	compressor
d	diffuser
dis	discharge
e	evaporator
exg	exergy
IHX	internal heat exchanger
j	ejector
k	condenser
n	nth state point
o	environment
pf	primary flow
sf	secondary flow
suc	suction
t	throttling valve

REFERENCES

[1] Shao Y, Xiao H, Chen B, Huang S, Qin FGF. 2018. Comparison and analysis of thermal efficiency and exergy efficiency in energy systems by case study. 5th International Conference on Energy and Environment Research (ICEER 2018); Prague, Czech Republic. p. 161-168. https://doi.org/10.1016/j.egypro.2018.10.081.

[2] Garcia JCS, Berana MS. 2020. Thermodynamic analysis and performance evaluation of a proposed novel combined cooling and power system. Philippine Engineering Journal. 41 (1): 1-18.

[3] Habka M, Ajib S. 2013. Determination and evaluation of the operation characteristics for two configurations of combined heat and power systems depending on the heating plant parameters in low-temperature geothermal applications. Energy Conversion and Management. 76: 996-1008.

[4] Wang J, Yang Y. 2016. Energy, exergy, and environmental analysis of a hybrid combined cooling, heating and power system utilizing biomass and solar energy. Energy Conversion and Management. 124: 566-577.

[5] Ustaoglu A, Kursuncu B, Alptekin M, Gok MS. 2020. Performance optimization and parametric evaluation of the cascade vapor compression refrigeration cycle using Taguchi and ANOVA methods. Applied Thermal Engineering. 180: 115816.

[6] Ustaoglu A. 2020. Parametric study of absorption refrigeration with vapor compression refrigeration cycle using wet, isentropic and azeotropic working fluids: conventional and advanced exergy approach. Energy. 201: 117491.

[7] Mohtaram S, Chen W, Lin J. 2017. Investigation on the combined Rankine-absorption power and refrigeration cycle using the parametric analysis and genetic algorithm. Energy Conversion and Management. 150: 754-762.

[8] Adebayo V, Abid M, Adedeji M, Dagbasi M, Bamisile O. 2021. Comparative thermodynamic performance analysis of a cascade refrigeration system with new refrigerants paired with CO2. Applied Thermal Engineering. 184: 116286.

[9] Akbari H, Sorin M. 2020. Thermal design and selection of the optimal working fluid for organic Rankine cycles based on the equivalent temperature concept. Applied Thermal Engineering. 168: 114860.

[10] Domanski PA, Yashar D, Kim M. 2005. Performance of a finned-tube evaporator optimized for different refrigerants and its effect on system efficiency. International Journal of Refrigeration. 28(6): 820-827.

[11] Allahyarzadeh-Bidgoli A, Dezan DJ, Yanagihara JI. 2020. COP optimization of propane pre-cooling cycle by optimal fin design of heat exchangers: efficiency and sustainability improvement. Journal of Cleaner Production. 271: 122585.

[12] Garcia JCS, Berana MS. 2017. Theoretical evaluation of the effect of internal heat exchanger in standard vapor compression and compressor-driven ejector refrigeration systems. World Congress on Engineering 2017; London, U.K.

[13] Rodriguez-Muñoz JL, Perez-Garcia V, Belman-Flores JM, Ituna-Yudonago JF, Gallegos-Muñoz A. 2018. Energy and exergy performance of the IHX position in ejector expansion refrigeration systems. International Journal of Refrigeration. 93: 122-131.

[14] Wei F, Senchuang G., Zhonghe H. 2019. Economic analysis of organic Rankine cycle (ORC) and organic Rankine cycle with internal heat exchanger (IORC) based on industrial waste heat source constraint. 10th International Conference on Applied Energy (ICAE2018); Hong Kong, China.

[15] Little AB, Garimella S. 2011. A review of ejector technology for refrigeration applications. International Journal of Air-Conditioning and Refrigeration. 19(1): 1-15.

[16] Yu M, Yu J. 2021. Thermodynamic analyses of a flash separation ejector refrigeration cycle with zeotropic mixture for cooling applications. Energy Conversion and Management. 229: 113755.

[17] Nehdi E, Kairouani L, Bouzaina M. 2007. Performance analysis of the vapor compression cycle using ejector as expander. International Journal of Energy Research. 31(4): 364-375.

[18] Sarkar J. 2009. Performance characteristics of natural-refrigerants-based ejector expansion refrigeration cycles. Proceedings of the Institution of Mechanical Engineers, Part A: Journal of Power and Energy. 223(5): 543-550.

[19] Li, H, Cao F, Bu X, Wang L, Wang X. 2014. Performance characteristics of R1234yf ejector-expansion refrigeration cycle. Applied Energy. 121: 96-103.

[20] Banasiak K, Hafner A, Andresen T. 2012. Experimental and numerical investigation of the influence of the two-phase ejector geometry on the performance of the R744 heat pump. International Journal of Refrigeration. 35(6): 1617-1625.

[21] Taslimi Taleghani S, Sorin M, Poncet S, Nesreddine H. 2019. Performance investigation of a two-phase transcritical CO2 ejector heat pump system. Energy Conversion and Management. 185: 442-454.

[22] Djuanda D. 2017. Performance study of double pipe internal heat exchanger in R-410a air conditioning system. International Conference on Thermal Science and Technology (ICTST) 2017; Bali, Indonesia. https://doi.org/10.1063/1.5046592.

[23] Moles F, Navarro-Esbri J, Peris B, Mota-Babiloni A, Barragan-Cervera A. 2014. Theoretical energy performance evaluation of different single stage vapor compression refrigeration configurations using R1234yf and R1234ze(E) as working fluids. International Journal of Refrigeration. 44: 141-150.

[24] Industrial Heat Pumps. Retrieved from http://industrialheatpumps.nl on 25 September 2019.
[25] Arpagaus C, Bless F, Uhlmann M, Schiffmann J, Bertsch SS. 2018. High temperature heat pumps: market overview, state of the art, research status, refrigerants, and application potentials. Energy. 152: 985-1010.
[26] Gas Servei. Retrieved from https://www.gas-servei.com/biblioteca/#documentacion on 25 September 2019.
[27] Brunin O, Feidt M, Hivet B. 1997. Comparison of the working domains of some compression heat pumps and a compression-absorption heat pump. International Journal of Refrigeration. 20(5): 308-318.
[28] Lemmon EW, Bell IH, Huber ML, McLinden MO. 2018. NIST Standard Reference Database 23: Reference Fluid Thermodynamic and Transport Properties – REFPROP, Version 10.0. National Institute of Standards and Technology, Standard Reference Data Program, Gaithersburg.